

## A RICH GLOBULAR CLUSTER SYSTEM IN DRAGONFLY 17: ARE ULTRA-DIFFUSE GALAXIES PURE STELLAR HALOS?

ERIC W. PENG<sup>1,2</sup> AND SUNGSOON LIM<sup>1,2</sup>

*Accepted for publication in The Astrophysical Journal Letters*

### ABSTRACT

Observations of nearby galaxy clusters at low surface brightness have identified galaxies with low luminosities, but sizes as large as  $L^*$  galaxies, leading them to be dubbed “ultra-diffuse galaxies” (UDGs). The survival of UDGs in dense environments like the Coma cluster suggests that UDGs could reside in much more massive dark halos. We report the detection of a substantial population of globular clusters (GCs) around a Coma UDG, Dragonfly 17 (DF17). We find that DF17 has a high GC specific frequency of  $S_N = 26 \pm 13$ . The GC system is extended, with an effective radius of  $12'' \pm 2''$ , or  $5.6 \pm 0.9$  kpc at Coma distance, 70% larger than the galaxy itself. We also estimate the mean of the GC luminosity function to infer a distance of  $97^{+17}_{-14}$  Mpc, providing redshift-independent confirmation that one of these UDGs is in the Coma cluster. The presence of a rich GC system in DF17 indicates that, despite its low stellar density, star formation was intense enough to form many massive star clusters. If DF17’s ratio of total GC mass to total halo mass is similar to those in other galaxies, then DF17 has an inferred total mass of  $\sim 10^{11} M_\odot$ , only  $\sim 10\%$  the mass of the Milky Way, but extremely dominated by dark matter, with  $M/L_V \approx 1000$ . We suggest that UDGs like DF17 may be “pure stellar halos”, i.e., galaxies that formed their stellar halo components, but then suffered an early cessation in star formation that prevented the formation of any substantial central disk or bulge.

*Subject headings:* galaxies: halos — galaxies: evolution — galaxies: star clusters: general — galaxies: stellar content — globular clusters: general

### 1. INTRODUCTION

The realm of low surface brightness is still one of the most unexplored in astronomy. Many of the visible counterparts to structures expected in a cold dark matter Universe are expected to be at a surface brightness much fainter than that of the night sky. A recent study using a new telescope optimized for low surface brightness imaging, the Dragonfly Telephoto Array, in conjunction with imaging from the Canada-France-Hawaii Telescope (CFHT), reported the discovery of 47 UDGs ( $\mu_{(e,g)} = 24\text{--}26$  mag arcsec<sup>-2</sup>) in the direction of the Coma cluster of galaxies (van Dokkum et al. 2015a). These galaxies have luminosities and appearances similar to early-type dwarf galaxies, but have much larger sizes, similar to  $L^*$  galaxies ( $1.5 < R_e < 4.5$  kpc). Their luminosities and sizes make them outliers in traditional scaling relation diagrams for galaxies. One UDG, DF44, has been confirmed to have a redshift consistent with membership in the Coma cluster (van Dokkum et al. 2015b). Subsequently, 854 new diffuse galaxies have been identified in Coma (Koda et al. 2015), and even lower surface brightness galaxies have been identified in the nearby Virgo cluster of galaxies (Mihos et al. 2015; Beasley et al. 2016) showing that these galaxies are far from uncommon, and that they may even be able to exist in the dense core of a galaxy cluster. Unfortunately, their low surface brightness and apparent lack of ongoing star formation makes it prohibitively difficult to study their stellar populations. Moreover, the distance of the Coma

cluster ( $\approx 100$  Mpc; Carter et al. 2008) puts resolved studies of their red giant branch (RGB) stars beyond the capabilities of current telescopes.

One probe of stellar populations that is within reach for these diffuse galaxies is globular clusters (GCs). GCs are old, compact star clusters whose presence in galaxies points to an early epoch of galaxy building where the intense star formation needed to form massive star clusters was commonplace. Observationally, they are useful tracers of old stellar populations because they can be observed at large distances. The number of GCs in a galaxy also correlates linearly with the total host halo mass (Blakeslee et al. 1997; Peng et al. 2008; Spitler & Forbes 2009; Harris et al. 2013), giving a way to estimate the total mass of a galaxy without other information. A recent study by Beasley et al. (2016) used kinematics of GCs in the Virgo cluster UDG VCC 1287 to show that the galaxy has an extremely high mass-to-light ratio, consistent with the premise that the number of GCs trace total mass, even in these extreme galaxies. The GC luminosity function peaks at a nearly universal luminosity, allowing an estimate of the distance to the galaxy. At the distance of the Coma cluster, GCs are readily visible in Hubble Space Telescope (*HST*) images.

We use archival *HST* Advanced Camera for Surveys Wide Field Channel (ACS/WFC) imaging of one Coma UDG, Dragonfly 17 (DF17), to investigate whether UDGs in the dense Coma cluster can host a system of GCs, and what that implies for the mass and origin of UDGs.

<sup>1</sup> Department of Astronomy, Peking University, Beijing 100871, China; peng@pku.edu.cn

<sup>2</sup> Kavli Institute for Astronomy and Astrophysics, Peking University, Beijing 100871, China

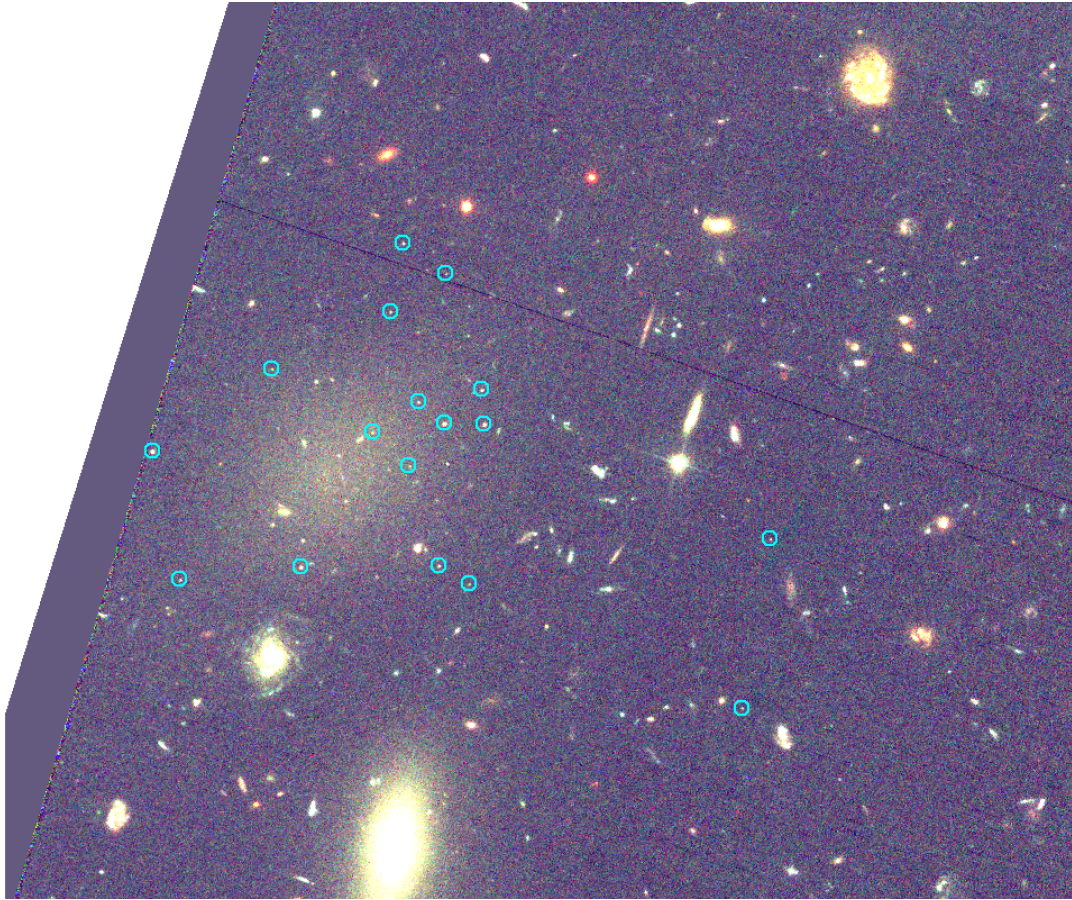


**Figure 1.** This  $68'' \times 57''$  image shows DF17 on the edge of the HST/ACS field of view. GC candidates (cyan circles) selected by morphology and color are clustered around the galaxy. The GCs roughly follow the star light, although there is some lopsidedness in the GCs, with nearly three times as many GCs on the NW side along the major axis than on the SE. There is no obvious evidence for a nuclear star cluster. North is up, and East is left.

## 2. OBSERVATIONS AND GLOBULAR CLUSTER CANDIDATE SELECTION

We used images taken with the *HST ACS/WFC* (GO-12476, PI: Cook, Macri et al. 2013). These data were described in (van Dokkum et al. 2015a), and are comprised of parallel observations in three filters ( $g_{475}$ ,  $V_{606}$ , and  $I_{814}$ ). We made deep stacked images using the AstroDrizzle task in DrizzlePac<sup>1</sup>. Total accumulated exposure times are 5100s, 5820s, and 5100s for the F475W, F606W, and F814W images, respectively. The pixel scale of the output images is  $0''.05/\text{pix}$ , and the full width at half maximum (FWHM) of point sources in the images is about two pixels.

We generated an object catalog using the Source Extractor (Bertin & Arnouts 1996) software package. For the detection image, we used a signal-to-noise ( $S/N$ )-weighted, combined image of all three filters. We performed aperture photometry within a  $0''.3$  diameter aperture, derived the aperture correction to a  $0''.5$  aperture using bright stars in the field, and then applied the aperture corrections to  $5''.5$  from Bohlin (2011).

GCs in the Coma cluster are unresolved, even with *HST*, so we first identified GC candidates as point sources. Similar to Peng et al. (2011), we defined an “inverse concentration” index ( $C_{4-7}$ ), which is the dif-

ference in magnitude between a 4-pixel aperture ( $0''.2$ ) and a 7-pixel aperture ( $0''.35$ ), normalized so that for point sources,  $C_{4-7} = 0$ . Although we detect objects as faint as  $V_{606} \approx 30$  mag, objects with  $V_{606} \gtrsim 29$  mag are overwhelmingly background sources, as the number counts of distant galaxies increases exponentially. For this reason, we define two GC candidate samples. The first is an “optimal” sample, which minimizes contamination and increases contrast between any GC population and the background. This sample has a flux limit of  $V_{606} < 28.25$  mag, and becomes increasingly stringent on the concentration criterion (removing more extended sources) for the faintest 2 mag. Our second sample is the “deep” sample, which has a simple flux limit of  $V_{606} < 29$  mag with symmetric cuts at  $\pm 0.1$  mag in concentration.

For both samples, we used the  $(g_{475} - V_{606})$  and  $(V_{606} - I_{814})$  colors to identify GC candidates by comparing objects in our field to the colors of GCs in the Virgo central galaxy, M87, which have HST/ACS photometry in the exact same filters (Peng et al. 2009; Jordán et al. 2009). We used the M87 GCs to define a locus in color space, and selected as GCs all objects whose  $2\sigma$  photometric uncertainty ellipse included the GC locus. This allows for more stringent selection for objects with more precise colors. We use the “optimal” sample for all subsequent analyses except for the measurement of the GC luminosity function (Section 3.2).

<sup>1</sup> [http://www.stsci.edu/hst/HST\\_overview/drizzlepac](http://www.stsci.edu/hst/HST_overview/drizzlepac)

## 3. RESULTS

3.1. *The GC system of DF17*

Figure 1 shows an image of DF17 with GC candidates from the “optimal” sample circled. The spatial distribution of GC candidates is highly concentrated toward DF17. The GC candidates roughly follow the stellar light of the galaxy, with a steep drop in numbers just beyond DF17’s optical radius. This strongly suggests that the GC candidates are physically associated with DF17. Within  $20''$  of the center of DF17 (a radius which contains all of the GC candidates clustered around the galaxy), we expect only 1.4 of the 15 selected objects to be background contaminants. This indicates that nearly all of the GC candidates around DF17 are, in fact, real GCs associated with the galaxy.

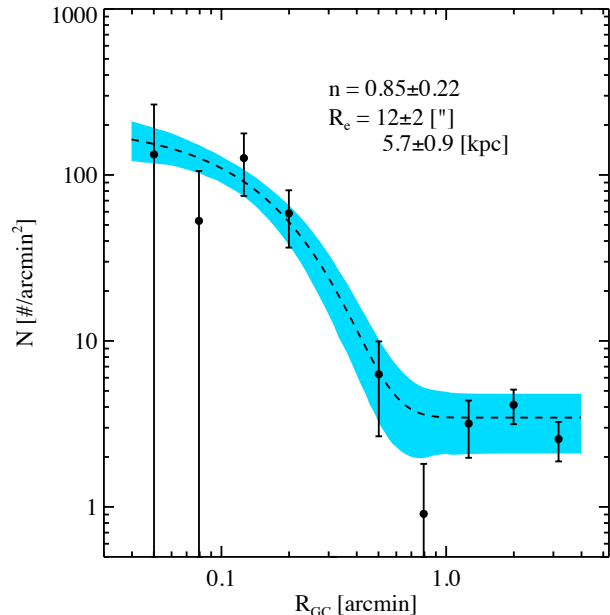
The GCs appear to be asymmetrically distributed about the galaxy, with nearly three times as many on the NW side along the major axis (which runs roughly NW-SE). Because DF17 is on the edge of the field of view, it is difficult to say whether this imbalance is mitigated at larger radii to the SE. We also note that there is no obvious nuclear star cluster above our detection limit.

Figure 2 shows the GC surface density profile. We characterize the profile using a Sersic function and constant background, with best-fit parameters estimated using maximum likelihood and bootstrap resampling. We find that the GC system has a profile consistent with a low Sersic index,  $n = 0.85 \pm 0.22$ , with a flat core and a steep outer drop off. The size of the GC system is characterized by the effective radius,  $R_{e,GC} = 12'' \pm 2''$ . For comparison, the effective radius measured for the stars from the same imaging is  $R_{e,stars} = 7''.0$  (van Dokkum et al. 2015a), so the GCs have an extent 70% larger than the already diffusely distributed stars, something which is also seen in more massive galaxies (e.g., McLaughlin 1999; Kartha et al. 2014).

3.2. *The GC Luminosity Function and the Distance to DF17*

The luminosity of the GCLF peak is a well-known distance indicator (e.g., Harris 2001), and measuring its apparent magnitude provides perhaps the only way to obtain a redshift-independent distance for such a distant UDG. At the distance of the Coma cluster ( $m - M \approx 35$ ), a GC system with a standard Gaussian luminosity function for a low-mass early-type galaxy (with mean  $M_V = -7.3$  mag; Miller & Lotz 2007) has a peak whose measurement is within the reach of these observations ( $V_0 \approx 27.7$  mag). Lee & Jang (2016) showed that GCLF distances to the Coma cluster can be obtained with HST imaging. For this analysis, we use our “deep” sample, which extends to  $V_{606} = 29$  mag.

We used artificial star tests to quantify the detection efficiency across our images. We used DAOPHOT II (Stetson 1987) to construct an empirical PSF using bright stars. We added artificial stars to images in all three filters, giving them a typical GC color, then ran the same detection and selection procedures as were used to generate the “deep” sample. The 90% completeness level is  $V_{606} = 28.1$  mag and the 50% completeness level is  $V_{606} = 28.8$  mag. This latter limit is fainter by  $\sim 1$  mag than the expected GCLF peak at the distance of Coma (see the dashed line in Figure 3).



**Figure 2.** The binned radial surface density profile of GCs in DF17 with best-fit Sersic profile overplotted. The profile has a flat core followed by a steep drop in the outer regions, which is consistent with a low Sersic index. The maximum likelihood estimates for the Sersic function parameters are  $n = 0.85 \pm 0.22$  and  $R_e = 12'' \pm 2''$ . The fit was performed directly on the unbinned data. For comparison, the Sersic fit for the stellar light in DF17 is  $n = 0.6$  and  $R_{e,stars} = 7''.0$ .

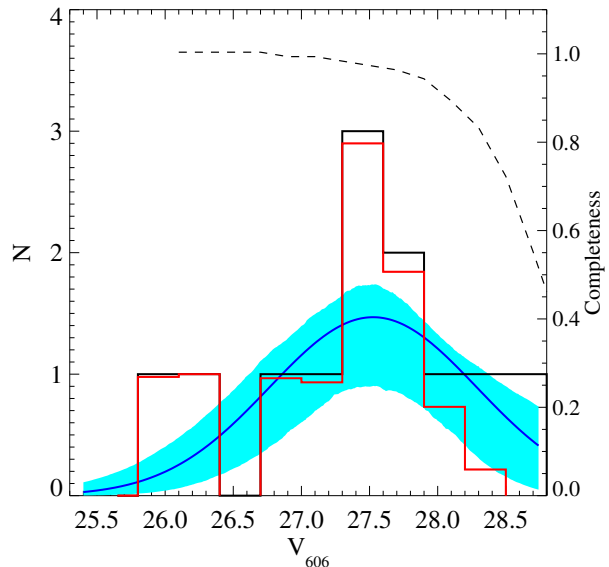


**Figure 3.** The GC luminosity function in DF17. We show the binned number counts of GC candidates (black histogram) and background-subtracted GC counts (red histogram) from our “deep” sample within the central  $12''$  ( $1R_{e,GC}$ ) of DF17. Overplotted is the best-fit Gaussian GCLF with  $\mu_{V_{606}} = 27.53 \pm 0.34$  and  $\sigma = 0.76 \pm 0.23$  (blue line) and the 68% confidence regions determined from the bootstrap (cyan). We also show the completeness of our observations as a function of  $V_{606}$  (dashed line). The observations are 90% complete  $1\sigma$  fainter than the GCLF peak. Assuming the peak of the GCLF in DF17 is similar to that in other nearby galaxies, DF17 is at a distance of  $97^{+17}_{-14}$  Mpc. The fit was performed on the unbinned data.



We used a Gaussian form for the GC luminosity function, a power law for the number counts of background sources (distant, unresolved galaxies), and multiplied both by the derived detection efficiency function. Using maximum likelihood estimation, we fit the normalization and power law slope of the background counts using the GC candidates outside a radius of  $36''$  ( $3R_{e,GC}$ ) from DF17, assuming that all of these objects are background objects. We fixed the power law model for the background to then estimate the Gaussian GCLF parameters for GC candidates within  $12''$ , the effective radius of the GC system. Figure 3 shows the number counts of GC candidates within the central  $12''$  of DF17, as well as the background-subtracted GC counts. *HST* resolution eliminates much of the background contamination at these magnitudes, and the small area in which the GCs reside also helps suppress contamination.

We find the best-fit parameters for the Gaussian GCLF to be  $\mu_{V_{606}} = 27.53 \pm 0.34$  mag and  $\sigma_{V_{606}} = 0.76 \pm 0.23$  mag. Figure 3 shows the best-fit Gaussian model, as well as the region that encompass 68% of the models fit using 1000 bootstrap resamples.

Because the  $V_{606}$  magnitude is not a standard  $V$ , we use transformations from DeGraaff et al. (2007, Equation 3) to convert the best-fit  $\mu_{V_{606}}$  to  $\mu_V$ . Using the color of a typical GC, we find that  $V - V_{606} = 0.13$  mag, and  $A_V = 0.025$  (Schlafly & Finkbeiner 2011), which results in the GCLF mean being  $\mu_{V_0} = 27.63 \pm 0.35$ . Assuming that the form of DF17’s GCLF is similar to those of nearby low-mass galaxies, this value of  $\mu_{V_0}$  places DF17 at a distance of  $97^{+17}_{-14}$  Mpc, putting it exactly in the Coma cluster.

### 3.3. Total Number of GCs and Specific Frequency

With our assumption of the form of the GCLF and the GC spatial density profile in DF17, we can estimate the total number of GCs. Counting seven GCs within  $R_e$  and brighter than the estimated GCLF mean, we find that  $N_{GC} = 28 \pm 14$  (where we include the uncertainty in the GCLF mean). DF17 has a luminosity of  $M_V = -15.1$  mag (using our distance and transforming from  $V_{606}$  reported in van Dokkum et al. 2015a), which gives a GC specific frequency of  $S_N = 26 \pm 13$ .

## 4. DISCUSSION

### 4.1. The Mass of DF17

DF17 has a substantial population of GCs, with a specific frequency ( $S_N = 26 \pm 13$ ) that is among the highest measured for any galaxy, and is the highest for its luminosity range. Figure 4 shows a compilation of high-quality, *HST*-derived  $S_N$  values for early-type galaxies (ETGs) across a range of luminosities. DF17 is a clear outlier at its luminosity, having a value of  $S_N$  only seen in galaxies two magnitudes fainter. Two extreme cases are VCC 1287 (Beasley et al. 2016), which has  $S_N \sim 80$ , and another ultra-diffuse galaxy in Virgo (Mihos et al. 2015) that has  $S_N \sim 40$ , but there are also low-mass galaxies with high  $S_N$  from Georgiev et al. (2010).

Work over the past couple decades has shown that the number of GCs in ETGs appears to be a reasonable estimator of the total mass of a galaxy or cluster (Blakeslee et al. 1997; McLaughlin 1999). As a result, the relationship between GC specific frequency (or GC stellar mass

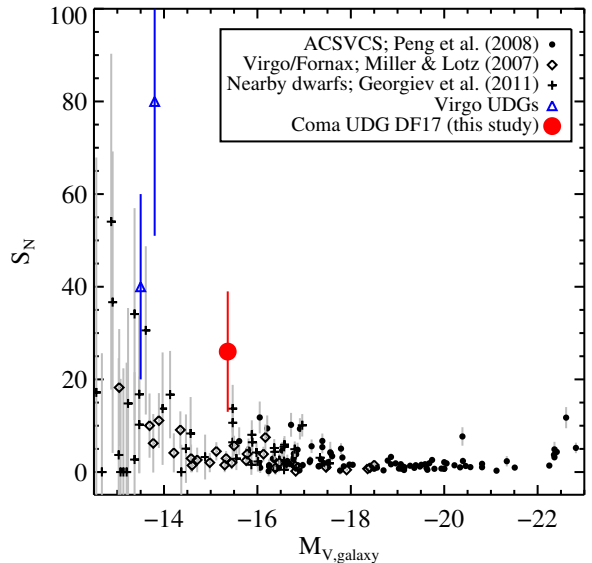


**Figure 4.** GC specific frequencies ( $S_N$ ) as a function of galaxy  $M_V$ . We plot  $S_N$  from three samples of galaxies with relatively high-precision  $S_N$  measurements, all derived from *HST* imaging: the Virgo cluster early-type galaxy sample from the ACSVCS (Peng et al. 2008, dots), the Virgo and Fornax cluster early-type dwarf galaxy sample of Miller & Lotz (2007, crosses), and the nearby low-mass galaxy sample of Georgiev et al. (2010, diamonds). We also plot the high- $S_N$  Virgo cluster ultra-diffuse galaxies from Mihos et al. (2015) and Beasley et al. (2016) (blue triangles). The Coma UDG from this study, DF17, is the red filled circle. For its luminosity, DF17 has a very high  $S_N$ , one which is only seen in galaxies at least two magnitudes fainter.

fraction) and galaxy stellar mass traces reasonably well the total mass–stellar mass relation for galaxies, both with a minimum around  $L^*$  (Peng et al. 2008; Spitler & Forbes 2009; Harris et al. 2013; Hudson et al. 2014). Provided that this relation holds across all galaxies, we can use the number of GCs in DF17 to estimate its total mass. We use the Harris et al. (2013) relation between the GC system mass and the total galaxy mass ( $M_{GCs}/M_{halo} = 6 \times 10^{-5}$ ) to determine a total mass for DF17 of  $(9.3 \pm 4.7) \times 10^{10} M_\odot$ , and a mass-to-light ratio of  $M/L_V \approx 1000$ . This total mass is roughly  $\sim 10\%$  that of the Milky Way.

The survival of UDGs in dense environments like Coma and other massive clusters (van der Burg et al. 2016) provides independent evidence that UDGs must be dark-matter dominated. Moreover, Beasley et al. (2016) used GC kinematics to find that the Virgo UDG, VCC 1287, has  $M/L \approx 3000$ , which was in line with what they inferred from their total number of GCs. These high mass-to-light ratios, and optical colors consistent with old stellar populations, suggest that tremendous gas loss (or lack of accretion) could have occurred early in the evolution of UDGs.

### 4.2. Ultra-Diffuse Galaxies as “Pure Stellar Halos”

The diffuseness of DF17’s stellar population seems to be at odds with the presence of GCs. Star clusters massive enough to be GC progenitors require intense star formation episodes, like those seen in gas-rich galaxy mergers. The existence of GCs require this kind of starburst in DF17, but a high star formation rate density

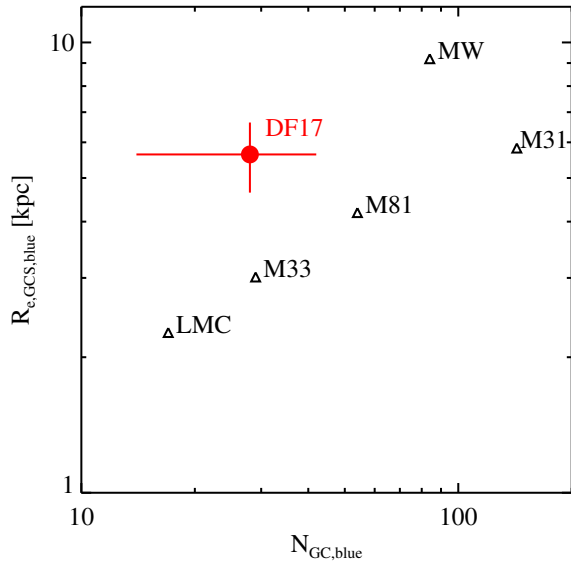


**Figure 5.** The half-number radii ( $R_e$ ) of the GC system versus of the total number of metal-poor (blue) GCs for DF17 compared to Local Group galaxies (Milky Way, M31, M33, and LMC) and the nearby spiral galaxy, M81 (Harris 1996; Caldwell et al. 2011; van den Bergh & Mackey 2004; San Roman et al. 2010; Fan & de Grijs 2014; Nantais & Huchra 2010). All the GCs in DF17 are assumed to be metal-poor. More massive GC systems are generally larger, and although the uncertainties are likely large for these galaxies, it appears that DF17’s GCs, like its stars, are in a more extended distribution than would be expected for its mass. Thus, its GC system is also ultra-diffuse.

should also produce a high surface brightness stellar component. Amorisco & Loeb (2016) suggested that UDGs could be the high angular momentum tail of the normal dwarf galaxy population. While their model produces the proper number of UDGs in clusters, it is unclear how such extended, low surface brightness (LSB) galaxies can produce massive star clusters. Present-day LSB disks, also thought to result from high angular momentum (Dalcanton et al. 1997), typically have little molecular gas and low star formation efficiencies (Bothun et al. 1997).

One way to explain a high  $S_N$  in a UDG is to posit that massive star clusters preferentially form earlier in a given star formation episode (e.g., Peng et al. 2008), and then the subsequent formation of field stars is rapidly quenched. This behavior is supported by measurements of  $[\alpha/Fe]$  in Virgo dwarf galaxies (Liu et al. 2016), in which dwarfs with higher  $S_N$  tend to have higher  $[\alpha/Fe]$ , suggesting a more rapid (and truncated) star formation history. In this scenario, DF17 should also have chemical abundance patterns typical of rapid star formation.

The constituents of DF17—an extended, spheroidal stellar population and a rich system of GCs—make it most similar to the stellar halos of normal galaxies. In effect, UDGs like DF17 are “pure stellar halos”: galaxies in which the old stellar halo forms, but then rapid gas removal and “starvation” prevents the formation of a more centrally concentrated disk or bulge component. Model decomposition of ETGs reveals the existence of extended, blue components with characteristic sizes of  $\sim 10$  kpc that may be the old stellar halo (Huang et al. 2013). Less massive disk galaxies like M33 also have

old stellar halos (McConnachie et al. 2010). If DF17 were to have a more “normal” specific frequency, keeping fixed the number of GCs, it would have a luminosity of  $M_V \approx -18$  to  $-19$  mag, comparable to that of M33.

In Figure 5, we compare the effective radius ( $R_e$ ) of the DF17 GC system to those of the metal-poor GC systems for the Milky Way, M31, M33, the LMC, and M81. We derive  $R_e$  for these galaxies using catalogs in the published literature (Harris 1996; Caldwell et al. 2011; van den Bergh & Mackey 2004; San Roman et al. 2010; Fan & de Grijs 2014; Nantais & Huchra 2010). These measurements are uncertain due to the inhomogeneous coverage and depths of the various surveys, but a trend is apparent where metal-poor GC systems with more GCs have larger sizes. DF17’s size stands out in this comparison, as its GC system has a size consistent with the more massive galaxies. However, its total number of GCs, and its total stellar mass, is significantly lower than those for the metal-poor stellar halos in the larger galaxies. We note that any subsequent central star formation would likely to move DF17 to the lower right (smaller size, more GCs) in this plot, in the direction of the other galaxies.

While the inferred mass of DF17 makes it unlikely that it is a “failed” Milky Way-like galaxy, DF17 could be the stellar halo of something less massive. A bright, relatively compact central stellar component in DF17 might look similar to a “normal”, sub- $L^*$  galaxy with a rather extended GC system. We speculate that ultra-diffuse galaxies like DF17 are analogous to the stellar halos of more luminous, high surface brightness galaxies, and that UDGs are part of the surviving population of proto-galaxies that built up the high- $S_N$ , high- $M/L$  stellar populations in the outskirts of today’s massive galaxies.

Our ability to detect GCs in UDGs out to the distance of the Coma cluster with *HST* gives us a relatively inexpensive way to estimate their total masses, distances, and study their star formation histories. Combined with the measurements of the extent of these GC systems, which can be compared to those of nearby galaxies, GCs will be a valuable resource to investigate the origins of UDGs.

EWP and SL acknowledge support from the National Natural Science Foundation of China under Grant No. 11573002, and from the Strategic Priority Research Program, “The Emergence of Cosmological Structures”, of the Chinese Academy of Sciences, Grant No. XDB09000105. Based on observations with the NASA/ESA Hubble Space Telescope obtained from the Mikulski Archive for Space Telescopes (MAST) at the Space Telescope Science Institute, which is operated by the Association of Universities for Research in Astronomy, Inc., under NASA contract NAS 5-26555. This research has made use of the NASA/IPAC Extragalactic Database (NED). This research made use of Astropy, a community-developed core Python package for Astronomy (Astropy Collaboration et al. 2013).

Facilities: HST(ACS)

## REFERENCES

Amorisco, N. C., & Loeb, A. 2016, MNRAS, 459, L51

- Astropy Collaboration, Robitaille, T. P., Tollerud, E. J., et al. 2013, *A&A*, 558, A33
- Beasley, M. A., Romanowsky, A. J., Pota, V., Navarro, I. M., Martinez Delgado, D., Neyer, F., & Deich, A. L. 2016, *ApJ*, 819, L20
- Bertin, E., & Arnouts, S. 1996, *A&AS*, 117, 393
- Blakeslee, J. P., Tonry, J. L., & Metzger, M. R. 1997, *AJ*, 114, 482
- Bohlin, R. C. 2011, Flux Calibration of the ACS CCD Cameras II. Encircled Energy Correction, Tech. rep.
- Bothun, G., Impey, C., & McGaugh, S. 1997, *PASP*, 109, 745
- Caldwell, N., Schiavon, R., Morrison, H., Rose, J. A., & Harding, P. 2011, *AJ*, 141, 61
- Carter, D., et al. 2008, *ApJS*, 176, 424
- Dalcanton, J. J., Spergel, D. N., & Summers, F. J. 1997, *ApJ*, 482, 659
- DeGraaff, R. B., Blakeslee, J. P., Meurer, G. R., & Putman, M. E. 2007, *ApJ*, 671, 1624
- Fan, Z., & de Grijs, R. 2014, *ApJS*, 211, 22
- Georgiev, I. Y., Puzia, T. H., Goudfrooij, P., & Hilker, M. 2010, *MNRAS*, 406, 1967
- Harris, W. E. 1996, *AJ*, 112, 1487
- Harris, W. E. 2001, in *Saas-Fee Advanced Course 28: Star Clusters*, ed. L. Labhardt & B. Binggeli, 223
- Harris, W. E., Harris, G. L. H., & Alessi, M. 2013, *ApJ*, 772, 82
- Huang, S., Ho, L. C., Peng, C. Y., Li, Z.-Y., & Barth, A. J. 2013, *ApJ*, 768, L28
- Hudson, M. J., Harris, G. L., & Harris, W. E. 2014, *ApJ*, 787, L5
- Jordán, A., et al. 2009, *ApJS*, 180, 54
- Kartha, S. S., Forbes, D. A., Spitler, L. R., et al. 2014, *MNRAS*, 437, 273
- Koda, J., Yagi, M., Yamanoi, H., & Komiyama, Y. 2015, *ApJ*, 807, L2
- Lee, M. G., & Jang, I. S. 2016, *ApJ*, 819, 77
- Liu, Y., et al. 2016, *ApJ*, 818, 179
- Macri, L. M., Hoffmann, S. L., Cook, K. H., Gregg, M., Mould, J. R., Stetson, P. B., & Welch, D. L. 2013, in *American Astronomical Society Meeting Abstracts*, Vol. 221, American Astronomical Society Meeting Abstracts #221, #152.06
- McConnachie, A. W., Ferguson, A. M. N., Irwin, M. J., Dubinski, J., Widrow, L. M., Dotter, A., Ibata, R., & Lewis, G. F. 2010, *ApJ*, 723, 1038
- McLaughlin, D. E. 1999, *AJ*, 117, 2398
- Mihos, J. C., et al. 2015, *ApJ*, 809, L21
- Miller, B. W., & Lotz, J. M. 2007, *ApJ*, 670, 1074
- Nantais, J. B., & Huchra, J. P. 2010, *AJ*, 139, 2620
- Peng, E. W., et al. 2008, *ApJ*, 681, 197
- . 2009, *ApJ*, 703, 42
- . 2011, *ApJ*, 730, 23
- San Roman, I., Sarajedini, A., & Aparicio, A. 2010, *ApJ*, 720, 1674
- Schlafly, E. F., & Finkbeiner, D. P. 2011, *ApJ*, 737, 103
- Spitler, L. R., & Forbes, D. A. 2009, *MNRAS*, 392, L1
- Stetson, P. B. 1987, *PASP*, 99, 191
- van den Bergh, S., & Mackey, A. D. 2004, *MNRAS*, 354, 713
- van der Burg, R. F. J., Muzzin, A., & Hoekstra, H. 2016, *ArXiv e-prints*
- van Dokkum, P. G., Abraham, R., Merritt, A., Zhang, J., Geha, M., & Conroy, C. 2015a, *ApJ*, 798, L45
- van Dokkum, P. G., et al. 2015b, *ApJ*, 804, L26